MICROSCOPY AND MICROANALYSIS

Microscopy Society of America

CAMBRIDGE UNIVERSITY PRESS

Spatial Distribution of Heterochromatin Bodies in the Nuclei of Triatoma infestans (Klug)

Journal:	*Microscopy and Microanalysis*
Manuscript ID	MAM-20-X-002.R1
Manuscript Type:	Original Article
Date Submitted by the Author:	n/a
Complete List of Authors:	Imperador, Carlos Henrique; University of Campinas, Institute of Biology, Dept Structural and Funcional Biology Bardella, Vanessa; UNESP, Department of Biology dos Anjos, Eli Heber; Universidade Estadual de Campinas - Campus Cidade Universitaria Zeferino Vaz, Dept Structural and Funcional Biology Rodrigues, Vera Lùcia; Superintendência de Controle de Endemias do Estado de São Paulo Cabral-de-Mello, Diogo; UNESP, Department of Biology Mello, Maria Luiza; University of Campinas, Institute of Biology, Dept Structural and Funcional Biology
Keywords:	confocal microscopy, chromatin topology, chromocenter, FISH, rDNA 18 S
Keywords:	confocal microscopy, chromatin topology, chromocenter, FISH, rDNA 18S
Abstract:	Constitutive heterochromatin typically exhibits low gene density and is commonly found adjacent or close to the nuclear periphery, in contrast to transcriptionally active genes concentrated in the innermost nuclear region. In Triatoma infestans cells, conspicuous constitutive heterochromatin forms deeply stained structures named chromocenters. However, to the best of our knowledge, no information exists regarding whether these chromocenters acquire a precise topology in the cell nuclei or whether their 18S rDNA, which is important for ribosome function, faces the nuclear center preferentially. In this work, the spatial

	distribution of fluorescent Feulgen-stained chromocenters and the distribution of their 18S rDNA were analyzed in Malpighian tubule cells of T. infestans using confocal microscopy. The chromocenters were shown to be spatially positioned relatively close to the nuclear periphery, though not adjacent to it. The variable distance between the chromocenters and the nuclear periphery suggests mobility of these bodies within the cell nuclei. The distribution of 18S rDNA at the edge of the chromocenters was not found to face the nuclear interior exclusively. Because the genome regions containing18S rDNA in the chromocenters also face the nuclear periphery, the proximity of the chromocenters to this nuclear region is not assumed to be associated with gene silencing.
Note: The following files were submitted by the author for peer review, but cannot be converted to PDF. You must view these files (e.g. movies) online.	
xMM Carlos Video 1 Triatoma 5 1 20.mp4 xMM Carlos Vídeo 2 Triatoma 5 1 20.mp4 xMM Carlos Vídeo 3 Triatoma 5 1 20.mp4	

Spatial Distribution of Heterochromatin Bodies in the Nuclei of *Triatoma infestans* (Klug)

Carlos Henrique L. Imperador[1], Vanessa B. Bardella[2], Eli Heber M. dos Anjos[1], Vera L.C.C. Rodrigues[3], Diogo C. Cabral-de-Mello[2] and Maria Luiza S. Mello[1]

[1] Department of Structural and Functional Biology, Institute of Biology, University of Campinas (Unicamp), Rua Monteiro Lobato 255, 13083-862 Campinas, SP, Brazil; carloshlimperador@gmail.com (C.H.L.I.); mlsmello@unicamp.br (M.L.S.M.); eliheber@unicamp.br (E.H.M.A.);
[2]Department of Biology, Institute of Biosciences, State University of São Paulo (Unesp), Avenida 24-A, 1515, 13506-900 Rio Claro, SP, Brazil; vbbardella@gmail.com (V.B.B.); mellodc@rc.unesp.br (D.C.C.M.);
[3]Superintendence for Control of Endemic Diseases (SUCEN), Rua Afonso Pessini, 86, 13845-206 Mogi-Guaçu, SP, Brazil; veracorrea@dglnet.com.br (V.L.C.C.R.)

Running head: Spatial Distribution of Heterochromatin

Author for correspondence: Maria Luiza S. Mello, E-mail: mlsmello@unicamp.br

Abstract

Constitutive heterochromatin typically exhibits low gene density and is commonly found adjacent or close to the nuclear periphery, in contrast to transcriptionally active genes concentrated in the innermost nuclear region. In *Triatoma infestans* cells, conspicuous constitutive heterochromatin forms deeply stained structures named chromocenters. However, to the best of our knowledge, no information exists regarding whether these chromocenters acquire a precise topology in the cell nuclei or whether their 18S rDNA, which is important for ribosome function, faces the nuclear center preferentially. In this work, the spatial distribution of fluorescent Feulgen-stained chromocenters and the distribution of their 18S rDNA were analyzed in Malpighian tubule cells of *T. infestans* using confocal microscopy. The chromocenters were shown to be spatially positioned relatively close to the nuclear periphery, though not adjacent to it. The variable distance between the chromocenters and the nuclear periphery suggests mobility of these bodies within the cell nuclei. The distribution of 18S rDNA at the edge of the chromocenters was not found to face the nuclear interior exclusively. Because the genome regions containing18S rDNA in the chromocenters also face the nuclear periphery, the proximity of the chromocenters to this nuclear region is not assumed to be associated with overall gene silencing.

#1

Key words: confocal microscopy, chromatin topology, chromocenter, FISH, heterochromatin, rDNA 18S

Introduction

Chromosomes are not randomly distributed within the cell nuclei (Ellison & Howard, 1981; Hochstrasser et al., 1986; Cryderman et al., 1999; Cremer et al., 2000, 2001; Olszewska et al., 2008; Jost et al., 2015). Even in the decondensed state of chromatin, it follows an organized distribution and certain nuclear positions within chromosome territories (Cremer & Cremer, 2001, 2010). Although the nucleus is not subdivided into compartments that are attached to its peripheral envelope, the regulatory machinery for transcription, replication and repair is organized into subnuclear domains with specific functions (Fritz et al., 2016).

Recent reports state that the spatial positioning of heterochromatin would be regulated such that it would be preferentially located at the nuclear periphery, whereas euchromatin would be positioned in the nuclear interior. In various cell types, this organization has been associated with gene density, with gene-rich chromosome territories and/or chromatin containing transcriptionally active genes occupying the nuclear interior, while gene-poor chromosome domains and/or chromatin with a relatively high amount of gene silencing are closer to the nuclear periphery (Croft et al., 1999; Küpper et al., 2007; Bártova et al., 2008; Boyle et al., 2011; Bickmore, 2013). However, this hypothesis has not been consistently supported either experimentally or simply based on descriptive terms (Kurz et al., 1996; Harnicarova et al., 2006; Finlan et al., 2008; Deniaud & Bickmore, 2009; Dieudonné et al., 2009; Solovei et al., 2009; Bickmore, 2013; Meister & Taddei, 2013). There are reports indicating that the nuclear periphery would not be refractory to genes and that it would participate in the modulation of certain genes in such a way that the repressive nature of the nuclear periphery would result from epigenetic modifications on histones (dimethylated- and trimethylated-lysine in histone H3, for instance) anchored in the nuclear envelope and leading to an increased concentration of silencing factors (Ruault et al., 2008; Towbin et al., 2009, 2013; Meister & Taddei, 2013). Therefore, the localization of heterochromatin, as is the case with the facultative type, when adjacent to the nuclear lamina (Ruault et al., 2008), would be associated with the perinuclear anchorage positioning of modified histones that would act on the epigenetic propagation of transcriptional repression (Towbin et al., 2013).

Regarding the spatial distribution of chromocenters that are constitutive heterochromatin bodies and that compartmentalize their components from the rest of the

genome, there is information indicating that the topology of chromocenters in certain organisms is not incidental. In the salivary glands of *Drosophila melanogaster*, for instance, one repetitive DNA-rich chromocenter is always positioned at the nuclear periphery and adhered to the nuclear envelope (Hochstrasser et al., 1986; Cryderman et al., 1999). It was proposed that this chromocenter participates in the control of the availability of repressive elements of the overall gene activity, such as proteins of the HP1 family (Cryderman et al., 1999). In early embryos of *D. virilis*, in which the chromocenter acquires the same position as in *D. melanogaster* (Ellison et al., 1981), it faces the exterior of the organism, whereas in the salivary glands of *D. melanogaster*, the chromocenter exhibits variable positions in relation to the organ lumen (Hochstrasser et al., 1986).

In plants such as *Arabidopsis thaliana*, the localization of 6 to 10 chromocenters that are rich in methylated DNA has also been reported to be close to the nuclear periphery (Franz et al., 2002; Fang & Spector, 2005; Berr & Schubert, 2007; De Nooijer et al., 2009). In human sperm cells, the centromeric and telomeric chromosome regions that constitute chromocenters acquire a nonrandom position. While the telomeres face the nuclear periphery, the centromeres face the nuclear center (Olszewska et al., 2008; Zalenskaya & Zalensky, 2004; Ioannou & Griffin, 2011; Alladin et al., 2013). There are reports indicating that changes in this topological pattern may be associated with male infertility (Ioannou & Griffin, 2011; Alladin et al., 2013).

In somatic cells of *Triatoma infestans*, which is one of the most important vectors of Chagas disease, chromocenters are highly conspicuous bodies (Mello, 1971, 1978) that are composed of at least three pairs of autosomes and sex chromosomes (Schreiber et al., 1972; Solari, 1979). These heterochromatin bodies contain AT-rich DNA (Alvarenga et al., 2011) and are circumscribed by the nucleolus (Mello et al., 1990). In the highly polyploid Malpighian tubule cell nuclei of *T. infestans*, one chromocenter is observed up to the 3rd nymphal instar; from this phase onward, a portion of the cells exhibit multichromocentered nuclei (Mello, 1971, 1978). This phenomenon is not associated with any known specific physiological change; the excretory function of the Malpighian tubules and the insect blood feeding processes do not change over the course of the insect's lifetime (Wigglesworth, 1984). Regarding the spatial distribution of these chromocenters, there is no conclusive information about whether it has a preferential or variable location inside the cell nuclei and whether it varies with insect development (Mello, 2013). In addition, there is no information on

whether a given gene positioned in the chromocenter surface or in contact with it would present a preferential position, facing only the nuclear interior. This knowledge would be relevant for a comparison with the spatial distribution of chromocenters in other cell systems, and for investigating whether these bodies contain an overall noncodifying chromatin (Mello, 1971).

In the present study, the spatial distribution of chromocenters in the cell nuclei of Malpighian tubule cells of *T. infestans* was investigated at various developmental phases. The chromocenter surface facing the nuclear interior was also investigated with regard to the positioning of 18S rDNA, which is part of an essential gene that acts in ribosome biogenesis. The chromocenters in nymphal and adult specimens were found to be positioned with relative proximity to the nuclear periphery, though not adjacent to it. Because of the relatively variable position of the chromocenters, they are thought to be susceptible to mobility inside the cell nuclei. The 18S rDNA sites placed on chromocenter regions that could face the nuclear interior and the nuclear periphery suggest that the proximity of the chromocenters to the nuclear periphery is not entirely a gene-silencing phenomenon.

Material and Methods

Insects

Male fifth instar nymphs and adults and third instar nymphs of an unknown sex of *Triatoma infestans* (Klug) were supplied by the insect facility of the Superintendence for Control of Endemic Diseases of the state of São Paulo (SUCEN) at Mogi-Guaçu (Brazil). These insects originated from natural populations of insects that have been collected in the north of the state of Minas Gerais (Vale do Jequitinhonha) (approximately between latitudes 16 °S and 18 °S and longitudes 41 °W and 43 °W) since 1980. In the SUCEN facility, the insects were fed chicken blood once every two weeks and reared at 30 °C and 80% relative humidity following the animal care and ethic procedures registered at the National Council of Animal Experimentation Control (COBEA) from the Brazilian Ministry of Science, Technology and Innovation under accreditation protocol no. 01200.003280/2014-28. The SUCEN Scientific and Ethics Committee approved this investigation (Protocol no. 64405/2015). Three to five specimens of each developmental stage were used for each assay.

Cell Fixation and Cytochemistry for Chromocenter Spatial Localization Using Confocal Microscopy

Whole-mounted Malpighian tubules were fixed in a mixture of absolute ethanol and glacial acetic acid (3:1, v/v) solution for 1 min, rinsed in 70% ethanol for 5 min and subjected to the fluorescent Feulgen reaction, which is a cytochemical assay specific for DNA (Mello & Vidal, 2017). The acid hydrolysis step of the Feulgen reaction was performed in 4 M HCl for 65 min at 25 °C (Mello et al., 2001). The Schiff reagent was diluted in sulfurous water (1:9, v/v). Following treatment with the Schiff reagent, the preparations were rinsed in three baths of sulfurous water (5 min each), rinsed in distilled water, air-dried, cleared in xylene for 10 min and mounted in VECTASHIELD® (Vector Laboratories, Burlingame, CA, USA). Malpighian tubules were used as the study organ because of their well-known cell biology, cytogenetics, fine structure and physiological and epigenetic characteristics (Mello, 1971, 1989; Mello & Dolder, 1977; Wigglesworth, 1984; Mello et al., 1995, 2001; Campos et al., 2002; Alvarenga et al., 2011, 2016).

Confocal Microscopy

The fluorescent images were examined using a Leica TS SP5 II broadband confocal microscope (Wetzlar, Germany) equipped with argonium and 543-nm and 633-nm helium-neonium lasers, 63-x and 100-x objectives, and the Leica Application Suite AF (Leica Microsystems) software at the LACTAD facilities (Unicamp, Campinas, Brazil). A spacing of 0.13 μm between optical sections was used for each nucleus. Because the nuclear size varies as a function of the insect developmental phase, further spacing compensation was performed with the software during the 3-D reconstruction. Twenty-six nuclei from 3rd instar nymphs, 69 nuclei (48 of which were single-chromocentered nuclei) from 5th instar nymphs and 30 nuclei (19 of which were single-chromocentered nuclei) from adults were analyzed.

Image Analysis and Statistics

The proximal (shorter) and distal (longer) axial distances between the chromocenters and the nuclear periphery were measured in the X, Y and Z axes using Image Pro-Plus 7 (Media Cybernetics, Inc.) software. A schematic representation of these axes is shown in Fig. 1. Comparisons were made through the Kruskal-Wallis and Mann-Whitney tests using Minitab 18™ (State College, PA, USA) software.

Fluorescence in Situ Hybridization (FISH): Probe Design, Hybridization and Detection

DNA was isolated from the leg muscles of four adult *T. infestans* specimens using the Wizard Genome DNA Purification kit (Promega, Madison, USA). The 18S rDNA fragments were amplified. The primer sets used for PCR were as follows: Sca 18SF (5' CCC CGT AAT CGG AAT GAG TA) and Sca 18SR (5' GAG GTT TCC CGT GTT GAG TC) (Cabral-de-Mello et al., 2010). The PCR products were labeled *via* nick-translation using biotin-14-dATP (Invitrogen, Carlsbad, USA). The Malpighian tubules of five 5th instar nymphs of *T. infestans* were fixed in an absolute ethanol-glacial acetic acid (3:1, v/v) solution for 1 min, squashed in a drop of 50% acetic acid aqueous solution, dehydrated in an ethanol series, and air-dried. The preparations were then subjected to treatment with 100 µg/mL RNase A (Sigma, St. Louis, MO, USA) for 1 h at 37°C, rinsed in a 2 x SSC solution for 10 min, postfixed in 4% formaldehyde for 10 min at room temperature and rinsed again in the 2 x SSC solution for 10 min. The samples were subsequently treated with 30 µL of the hybridization mixture, which contained 100 ng of the labeled probe, followed by denaturation/renaturation cycles and posthybridization rinses. The detailed protocol was previously described (Pinkel et al., 1986; Alvarenga et al., 2018). The probe was detected using a solution composed of 5 µg/mL streptavidin-Alexa Fluor 488 conjugate (Invitrogen) and 5% BSA/4SSC/0.2% Tween 20 (1:100, v/v) for 1 h in a moist chamber. Then, the preparations were rinsed in 4-x SSC/0.2% Tween 20 at room temperature, counterstained with DAPI and mounted in VECTASHIELD® (Vector Laboratories).

FISH: Ordinary Fluorescence Microscopy

The nuclear images of at least 20 nuclei were captured (12 of which were single-chromocentered nuclei) using an Olympus BX61 microscope equipped with the

appropriate filters and a DP70 digital camera. Image merging was performed using Adobe Photoshop CS5.

FISH: Confocal Microscopy

3-D observations were made using a Leica TS SP5 II broadband confocal microscope (Wetzlar, Germany) equipped with argonium and helium-neonium lasers, 63-x and 100-x objectives, and the Leica Application Suite AF (Leica Microsystems) software. At least 20 nuclei were examined.

Results

Chromocenter Topology

The chromocenters of the single- and multichromocentered nuclei in the Feulgen-stained Malpighian tubules of *T. infestans* consistently presented a deeper fluorescence in comparison with euchromatin (Fig. 2). All the examined nuclei exhibited an ellipsoidal shape with a shorter nucleus axis in the Z-coordinate, and the diameters of the X- and Y-axes differing from each other (Fig. 3; Table 1 and Suppl. Table S1). Examples of the nuclear images, image gallery and 3D-nuclear reconstitution of the Feulgen-stained preparations are shown in Supplementary Figs. S1-S3 and Video 1. The nuclei of the adult specimens are similar to those of the 5th instar nymphs. The measurements taken using confocal microscopy demonstrated a tendency of the chromocenters to be close to the nuclear periphery based on the significant difference in the proximal and distal distances between the chromocenters and the nuclear periphery (Fig. 3; Table 1). However, there is no strict contiguity between the chromocenters and the nuclear periphery.

The values of the proximal and distal distances between the chromocenters and the nuclear periphery in the X-, Y- and Z-axes were highly variable (Table 1). These distances in the X- and Y-axes increase along nymphal development (Fig. 3, Table 1 and Suppl. Table S2), but those in the adult phase and the 5th nymphal instar do not differ from each other with the exception of the distance in the Y-axis in single-chromocentered nuclei (Suppl. Table S2). In the Z-axis, the proximal and distal distances between the chromocenters and the nuclear periphery do not significantly

change with the progress of nymphal development but they increase in the single-chromocentered nuclei of the adult specimens (Table 1 and Suppl. Table S2).

The nuclear diameters in the X- and Y-axes also increase with the progress of nymphal development, but they decrease slightly in the adult phase (Table 1 and Suppl. Table S2). The nuclear diameter in the Z-axis increases with the progress of nymphal development but it does not change in the adult phase (Table 1 and Suppl. Table S2).

18S rDNA Sites

The fluorescent signals for 18S rDNA examined using fluorescence microscopy followed by observations with confocal microscopy (Fig. 4a, b) and 3-D reconstitution (Videos 2 and 3), were more intense on the surface of the chromocenters. In other nuclear areas, fluorescent signals were also observed and, in certain cases, corresponded to heterochromatic corpuscles that were apparently budding from the large chromocenter body, where multichromocentered bodies were in the process of formation (Video 3). The fluorescent signals on the chromocenter areas face not only the interior but also the periphery of the cell nuclei (Videos 2 and 3).

Discussion

Because the fluorescent Feulgen reaction permits the identification, localization and quantification of DNA (Mello & Vidal, 2017), the distribution of global chromatin and of the heterochromatic bodies that constitute chromocenters in the nuclei of the Malpighian tubules of *T. infestans* could be adequately analyzed using confocal microscopy. The red fluorescence emitted by chromatin apurinic acid using the Feulgen reaction against the black background enables efficient establishment of the nuclear periphery.

The morphometric results obtained in the present work demonstrated a tendency of the chromocenters to locate with proximity to the nuclear periphery during the nymphal stages and adult phase, as the proximal and distal distances between the chromocenters and the nuclear periphery differed especially in the X- and Y-optical axes. The proximity of the chromocenters to the nuclear periphery, as assessed using confocal microscopy, is consistent with images obtained using ordinary microscopy observations of nonfluorescent Feulgen-stained cells (Suppl. Fig. S4a) and electron

microscopy images, one of which is shown in Supplementary Fig. S4b. Previous data using a mathematical descriptor (AD^2 = average square distance) after computation of absorbances obtained using a Zeiss Universal double-beam automatic scanning microspectrophotometer (UMSP-I, University of Freiburg, Germany) demonstrated that the chromocenter areas come farther from the center of the nuclear image in Malpighian tubule cells of 4th and 5th instar nymphs of *T. infestans* (Mello, 1978). The AD^2 descriptor compares the peripheral property of a given collection of points before and after "cleaning" of the absorbances of noncondensed chromatin areas using Moore's squares ratio method which searches for the maximal contrast cutoff point for distinguishing heterochromatin from euchromatin (Vidal et al., 1973). #1 #2

The present confocal microscopy results are also consistent with reports of other organisms although in such cases, the chromocenters appeared adjacent or considerably closer to the nuclear envelope (Ellison & Howard, 1981; Hochstrasser et al., 1986; Cryderman et al., 1999; Fransz et al., 2002; Fang & Spector, 2005; Berr & Schubert, 2007; De Nooijer et al., 2009). #1

The fact that the proximal and distal distances between the chromocenters and the nuclear periphery increased with nymphal development, whereas these distances remained constant in the adult stage, is likely related to the increased polyploidy that is demonstrated in the Malpighian tubule cell nuclei during nymphal development; the doubling of the DNA content ceases in adult individuals (Mello, 1971, 1975, 1978). When these distances continue to increase or even decrease in adult specimens, such factors as a variable presence of nonhistone proteins and/or rRNA transcripts due to functional requirements, may be responsible. Variable hydration levels are also known to contribute to the nuclear volume (Mello, 1972).

Considering that there is variability in proximal and distal distances between the chromocenters and the nuclear edge in the studied developmental phases and the adult stage of the Malpighian tubules of *T. infestans,* it is hypothesized that the chromocenters may exhibit movement within the cell nuclei. This phenomenon might occur due to the physical pressure exerted by the euchromatin mass and/or the variability in the HP1-α content or nucleolar masses that have been reported to occur associated with these heterochromatic bodies (Mello et al., 1990; Alvarenga et al., 2016). Clearly, to demonstrate that chromocenter motions occur within the nuclei *in vivo* observations monitored by microcinematography may be relevant.

Although the euchromatin in the Malpighian tubules of *T. infestans* exhibits acetylation of lysine 9 in histone H3 (H3K9ac) and lysine 8 and 16 in histone H4 (H4K8ac and H4K16ac), as well as mono- and di-methylation of lysine 9 in histone H3 (H3K9me and H3K9me$_2$) and lysine 20 in histone H4 (H4K20me and H4K20me$_2$), these epigenetic marks have not been encountered in chromocenters (Alvarenga et al., 2016). However, the H3K9ac, H4K8ac and H3K9me marks were shown to be concentrated around the chromocenter in single-chromocentered nuclei (Alvarenga et al., 2016). This report leads to the hypothesis that in the chromocenter periphery or in the euchromatin in close contact with the chromocenter, transcriptional activity may occur, as several authors have described the enrichment in these marks in the promoters of active genes (Sterner & Berger, 2000; Talasz et al., 2005; Wu et al., 2005; Bártova et al., 2008). Particularly in *T. infestans*, these marks may be related to rDNA transcription, as the nucleolar mass closely circumscribes the chromocenter(s) (Mello et al., 1990). This hypothesis was confirmed by the present FISH results, as assessed using confocal microscopy and 3-D image videos, in which 18S rDNA signals were revealed in the periphery of the chromocenter(s). During the formation of multichromocentered nuclei, when small chromocenters bud from a large chromocenter body, the 18S rDNA signals follow the surface of all these structures.

According to Pita et al. (2017), the lineage of *T. infestans* currently found in Brazil has an Andean origin. In this lineage, chromatin regions containing 45S rDNA are assumed to occur in only one of the large autosome pairs; in contrast, in the non-Andean lineage, these regions would be present in the X sex chromosomes (Panzera et al., 2012). The large A, B and C autosome pairs and the X and Y sex chromosomes form the chromocenters of *T. infestans* (Schreiber et al., 1972; Solari, 1979). Therefore, regardless of the evolutionary origin of the *T. infestans* specimens analyzed in the present work, the nucleolus organizer region containing the 18S rDNA is assumed to compose part of their chromocenter(s) while also being distributed in various points of chromatin outside of the chromocenters. The integration of the nucleolus organizer in the chromocenter(s) could be concluded after a genomic analysis of the structure isolated through microdissection, which is a matter for further investigation.

In conclusion, the position that the chromocenters of *T. infestans* occupy within Malpighian tubule cell nuclei is nonrandomly distributed and it may be susceptible to dynamic motions. Genome regions containing 18S rDNA appear to be distributed in the periphery of these chromocenters. Despite the relative proximity of the chromocenters

#1

to the nuclear periphery, there is no association of a relevant gene locus for cell function as that of the 18S rDNA facing a preferential central or peripheral nuclear position. Because genome regions containing 18S rDNA were also present in chromocenter regions facing the nuclear periphery, the proximity of the chromocenters to this nuclear region is not assumed to be associated with an overall gene silencing. What triggers a chromocenter heterochromatin, such as that of *T. infestans*, to nuclear peripheric sites and enables transcription at the chromocenters' periphery are still unanswered questions as noted recently by Allshire and Madhani (2018).

#2

Acknowledgments. This research was supported by the São Paulo State Research Foundation (FAPESP, Brazil; grant no. 2015/10356-2) and the Brazilian National Council for Research and Development (CNPq, grant no. 304668/2014-1). The funders had no role in study design, data collection and analysis, decision to publish, or preparation of the manuscript. C.H.L.I. received a fellowship from the Coordenação de Aperfeiçoamento de Pessoal de Nível Superior (CAPES, Brazil – Finance Code 001). M.L.S.M. received a fellowship from CNPq (grant no. 304668/2014-1).

Authors' Contributions. M.L.S.M. conceived and designed the experiments. C.H.L.I, V.B.B., E.H.M.A. and V.L.C.C.R. performed the experiments. C.H.L.I., V.B.B. and M.L.S.M. analyzed the data. M.L.S.M. and D.C.C.-de-M. contributed the reagents/materials/analysis tools. M.L.S.M. supervised the study. M.L.S.M. and D.C.C.-de-M. wrote the original draft of the manuscript. All authors read and approved the final manuscript.

References

Alladin N, Moskovtsev SI, Russel H, Kenigsberg S, Lulat, AGM, Librach CL (2013) The three-dimensional image analysis of the chromocenter in motile and immotile human sperm. *Systems Biol Reprod Med* **59**, 146-152. (https//doi.org/10.3109/19396368.2013.772679)

Allshire RC, Madhani HD (2018) Ten principles of heterochromatin formation and function. *Nature Rev* **19**, 229-244. (doi: 10.1038/nrm.2017.119)

Alvarenga EM, Imperador CHL, Bardella VB, Rodrigues VLCC, Mondin M, Cabral-de-Mello DC, Moraes AS, Mello MLS (2018) Histone acetylation and

methylation marks in chromatin of *Panstrongylus megistus* (Hemiptera, Reduviidae). *Acta Histochem* **120**, 572-577. (http://dx.doi.org/10.1016/j.acthis.2018.07.002)

Alvarenga EM, Mondin M, Martins JA, Rodrigues VLCC, Vidal BC, Rincones J, Carazzolle MF, Andrade LM, Mello MLS (2011) Spatial distribution of AT- and GC-rich DNA within interphase cell nuclei of *Triatoma infestans* Klug. *Micron* **42**, 568-578. (https://dx.doi.org/10/1016/j.micron.2011.02.002)

Alvarenga EM, Rodrigues VLCC, Moraes AS, Naves LS, Mondin M, Felisbino MB, Mello MLS (2016) Histone epigenetic marks in heterochromatin and euchromatin of the Chagas' disease vector, *Triatoma infestans*. *Acta Histochem* **118**, 401-412. (http://dx.doi.org/10.1016/j.acthis.2016.04.002)

Bártova E, Krejci J, Harnicarová A, Galiová G, Kozubek S (2008) Histone modifications and nuclear architecture: A review. *J Histochem Cytochem* **56**, 711-721. (https://doi.org/10.1369/jhc.2008.951251)

Berr A, Schubert I (2007) Interphase chromosome arrangement in *Arabidopsis thaliana* is similar in differentiated and meristematic tissues and shows a transient mirror symmetry after nuclear division. *Genetics* **176**, 853-863. (https://doi.org/10.1534/genetics.107.073270)

Bickmore WA (2013) The spatial organization of the human genome. *Ann Rev Genomics Human Genet* **14**, 67-84. (http://doi.org/10.1146/annurev-genom-091212-153515)

Boyle S, Rodesch MJ, Halvensleben HA, Jeddeloh JA, Bickmore WA (2011) Fluorescence in situ hybridization with high-complexity repeat-free oligonucleotide probes generated by massively parallel synthesis. *Chromosome Res* **19**, 901-909. (https://doi.org/10.1007/s10577-011-9245-0)

Cabral-de-Mello DC, Moura RC, Martins C (2010) Chromosomal mapping of repetitive DNAs in the beetle *Dichotomius geminatus* provides the first evidence for an association of 5S rRNA and histone H3 genes in insects, and repetitive DNA similarity between the B chromosome and a complement. *Heredity* **104**, 393-400. (https://doi.org/10.1038/hdy.2009.126)

Campos SGP, Rodrigues VLCC, Mello MLS (2002) Changes in nuclear phenotype frequencies following sequential cold shocks in *Triatoma infestans* (Hemiptera, Reduviidae). *Mem Inst Oswaldo Cruz* **97**, 857-864.

Cremer M, von Hase J, Volm T, Brero A, Kreth G, Walter J, Fischer C, Solovei I, Cremer C, Cremer T (2001) Non-random radial higher-order chromatin arrangements in nuclei of diploid human cells. *Chromosome Res* **9**, 541-567. (https://doi.org/10.1023/A:1012495201697)

Cremer T, Cremer C (2001) Chromosome territories, nuclear architecture and gene regulation in mammalian cells. *Nature Rev Genet* **2**, 292-301. (https://doi.org/10.1038/35066075)

Cremer T, Cremer C (2010). Chromosome Territories. Cold Spring Harbor Perspective in Biology, pp. 1-23.

Cremer T, Kreth G, Koester H, Fink RH, Heintzmann R, Cremer M, Solovei I, Zink D, Cremer C (2000) Chromosome territories, interchromatin domain compartment, and nuclear matrix: an integrated view of the functional nuclear architecture. *Crit Rev Eukaryot Gene Expr* **10**, 179-212. (https://doi.org/10.1615/CritRevEukarGeneExpr.v10.i2.60)

Croft JA, Bridger JM, Boyle S, Perry P, Teague P, Bickmore WA (1999) Differences in the localization and morphology of chromosomes in the human nucleus. *J Cell Biol* **145**, 1119-1131. (https://doi.org/10.1083/jcb.145.6.1119)

Cryderman DE, Morris EJ, Biessmann H, Elgin SCR, Wallrath LL (1999) Silencing at *Drosophila* telomeres: nuclear organization and chromatin structure play critical roles. *EMBO J* **18**, 3724-3735. (https://doi.org/10.1093/emboj/18.13.3724)

De Nooijer S, Wellink J, Mulder B, Bisseling T (2009) Non-specific interactions are sufficient to explain the position of heterochromatic chromocenters and nucleoli in interphase nuclei. *Nucleic Acids Res* **37**, 3558-3568. (https://doi.org/10.1093/nar/gkp219)

Deniaud E, Bickmore WA (2009) Transcription and the nuclear periphery: edge of darkness? *Curr Op Genet Dev* **19**, 187-191. (https://doi.org/10.1016/j.gde.2009.01.005)

Dieudonné M, Maiuri P, Biancotto C, Knezevich A, Kula A, Lusic M, Marcello A (2009) Transcriptional competence of the integrated HIC-1 provirus at the nuclear periphery. *EMBO J* **28**, 2231-2243. (https://doi.org/10.1038/emboj.2009.141)

Ellison JR, Howard GC (1981) Non-random position of the AT-rich DNA sequences in early embryos of *Drosophila virilis*. *Chromosoma* **83**, 555-561. (https://doi.org/10.1007/BF00328279)

Fang Y, Spector D (2005) Centromere positioning and dynamics in living *Arabidopsis* plants. *Mol Biol Cell* **16**, 5710-5718. (https://doi.org/10.1091/mbc.e05-08-0706)

Finlan LE, Sproul D, Thomson I, Boyle S, Kerr E, Perry P, Ylstra B, Chubb JR, Bickmore WA (2008) Recruitment to the nuclear periphery can alter expression of genes in human cells. *PLoS Genet* **4**, e1000039. (https://doi.org/10.1371/journal.pgen.1000039)

Fransz P, De Jong J, Lysak M, Castiglione MR, Schubert I (2002) Interphase chromosomes in *Arabidopsis* are organized as well defined chromocenters from which euchromatin loops emanate. *Proc Natl Acad Sci USA* **99**, 14584-14589. (https://doi.org/10.1073/pnas.212325299)

Fritz A, Baructu AR, Martin-Buley L, van Wijnen AJ, ZaidiS.K, Imbalzano AN, Lian JB, Stein JL, Stein GS (2016) Chromosomes at work: Organization of chromosome territories in the interphase nucleus. *J Cell Biochem* **117**, 9-19. (https://doi.org/10.1002/jcb.25280)

Harnicarova A, Kozubek S, Pachernik J, Krejci J, Bártova E (2006) Distinct nuclear arrangement of active and inactive c-*myc* genes in control and differentiated colon carcinoma cells. *Expt Cell Res* **312**, 4019-4035. (https://doi.org/10.1016/j.yexcr.2006.09.007)

Hochstrasser M, Mathog D, Gruenbaum Y, Saumweber H, Sedat JW (1986) Spatial organization of chromosomes in the salivary gland nuclei of *Drosophila melanogaster*. *J Cell Biol* **102**, 112-123. (https://doi.org/10.1083/jcb.102.1.112)

Ioannou D, Griffin DK (2011) Male infertility, chromosome abnormalities, and nuclear organization. *Cytogenet Genome Res* **133**, 269-279. (https://doi.org/10.1159/000322060)

Jost KL, Bertulat B, Rapp A, Brero A, Hardt T, Domaing P, Gösele C, Schulz H, Hübner N, Cardoso MC (2015) Gene repositioning within the cell nucleus is not random and is determined by its genomic neighborhood. *Epigenet Chromatin* **8**, 36. ((https://doi.org/10.1186/s13072-015-0025-5)

Küpper K, Kölbl A, Biener D, Dittrich S, von Hase J, Thormeyer T, Fiegler H, Carter NP, Speicher MR, Cremer T, Cremer M (2007) Radial chromatin positioning is shaped by local gene density, not by gene expression. *Chromosoma* **116**, 285-306. (https://doi.org/10.1007/s00412-007-0098-4)

Kurz A, Lampel S, Nickolenko JE, Bradl J, Benner A, Zirbel RM, Cremer T, Lichter P (1996) Active and inactive genes localize preferentially in the periphery

of chromosome territories. *J Cell Biol* **135**, 1195-1205. (https://doi.org/10.1083/jcb.135.5.1195)

Meister P, Taddei A (2013) Building silent compartments at the nuclear periphery: A recurrent theme. *Curr Op Genet Dev* **23**, 96-103. (https://doi.org/10.1016/j.gde.2012.12.001)

Mello MLS (1971) Nuclear behavior in the Malpighian tubes of *Triatoma infestans*. *Cytologia (Tokyo)* **36**, 42-49. (https://doi.org/10.1508/cytologia.36.42)

Mello MLS (1972) Micro-interferometry of insect polyploidy nuclei. *Cytologia (Tokyo)* **37**, 261-270. (https://doi.org/10.1508/cytologia.37.261)

Mello MLS (1975) Feulgen-DNA values and ploidy degrees in the Malpighian tubes of some triatomids. *Rev Brasil Pesq Méd Biol* **8**, 101-107.

Mello MLS (1978) Computer analysis of stained chromatin in Malpighian tubes of *Triatoma infestans* (Klug) (Hemiptera, Reduviidae). *Mikroskopie (Wien)* **34**, 285-299.

Mello MLS (1989) Nuclear fusion and change in chromatin packing state in response to starvation in *Triatoma infestans*. *Rev Brasil Genét* **12**, 485-498.

Mello MLS (2013) Spatial distribution of heterochromatin bodies in vectors of Chagas disease as studied by confocal microscopy. Proc Micr Conference MC 2013, Regensburg, pp. 131-132.

Mello MLS, Dolder H (1977) Fine structure of the Malpighian tubes in the blood-sucking insect, *Triatoma infestans* Klug. *Protoplasma* **93**, 275-288. (https://doi.org/10.1007/BF01275659)

Mello MLS, Vidal BC (2017) The Feulgen reaction: A brief review and new perspectives. *Acta Histochem* **119**, 603-609. (https://dx.doi.org/10.1016/j.acthis.2017.07.002)

Mello MLS, Dolder H, Dias CA (1990) Nuclear ultrastructure of Malpighian tubule cells in *Triatoma infestans* (Hemiptera, Reduviidae) under conditions of full nourishment and starvation. *Rev Brasil Genét* **13**, 5-17.

Mello MLS, Kubrusly FS, Randi MAF, Rodrigues VLCC, Ferraz-Filho NA (1995) Effects of heavy metals on chromatin supraorganization, nuclear phenotypes, and survival of *Triatoma infestans*. *Entomol Exp Appl* **74**, 209-218. (http://doi.org/10.1111/j.1570-7458.1995.tb01893.x)

Mello MLS, Tavares MCH, Dantas MM, Rodrigues VLCC, Maria SS, Campos SP, Garcia NL (2001) Cell death and survival alterations in Malpighian tubules of

Triatoma infestans following heat shock. *Biochem Cell Biol* **79**, 709-717. (https://doi.org/10.1139/o01-136)

Olszewska M, Wiland E, Kurpisz M (2008) Positioning of chromosome 15, 18, X and Y centromeres in sperm cells of fertile individuals and infertile patients with increased level of aneuploidy. *Chromosome Res* **16**, 875-890. (https://doi.org/10.1007/s10577-008-1246-2)

Panzera Y, Pita S, Ferreiro MJ, Ferrandis I, Lages C, Pérez R, Silva AE, Guerra M, Panzera F (2012) High dynamics of rDNA cluster location in kissing bug holocentric chromosomes (Triatominae, Heteroptera). *Cytogenet Genome Res* **138**, 56-67. ((https://doi.org/10.1159/000341888)

Pinkel D, Straume T, Gray JW (1986) Cytogenetic analysis using quantitative, high-sensitivity, fluorescence hybridization. *Proc Natl Acad Sci USA* **83**, 2934-2938. (https://doi.org/10.1073/pnas.83.9.2934)

Pita S, Panzera F, Mora P, Vela J, Cuadrado Á, Sánchez A, Palomegue T, Lorite P (2017) Comparative repeatome analysis on *Triatoma infestans* Andean and non-Andean lineages, main vector of Chagas disease. *PLoS ONE* **12**, e0181635. ((https://doi.org/10.1371/journal.pone.0181635)

Ruault M, Dubarry M, Taddei A (2008) Re-positioning genes in the nuclear envelope in mammalian cells: impact on transcription. *Trends Genet* **24**, 574-581. (https://doi.org/10.1016/j.tig.2008.08.008)

Schreiber G, Bogliolo AR, Pinto AC (1972) Cytogenetics of Triatominae: caryotype, DNA content, nuclear size and heteropyknosis of autosomes. *Brazil J Biol* **32**, 255-263.

Solari J (1979) Autosomal synaptonemal complexes and sex chromosomes without axes in *Triatoma infestans* (Reduviidae: Hemiptera). *Chromosoma* **72**, 225-240. (https://doi.org/10.10007/BF00293236)

Solovei I, Kreysing M, LanctôtC., Kösem S, Peichl L, Cremer T, Gick J, Joffe B (2009) Nuclear architecture of rod photoreceptor cells adapts to vision in mammalian evolution. *Cell* **137**, 356-368. (https://doi.org/10.1016/j.cell.2009.01.052)

Sterner DE, Berger SL (2000) Acetylation of histones and transcription-related factors. *Microbiol Mol Biol Rev* **64**, 435-459. (https://doi.org/10.1128/MMBR.64.2.435-459.2000)

Talasz H, Lindner HH, Sarg B, Helliger W (2005) Histone H4-lysine 20 monomethylation is increased in promoter and coding regions of active genes and correlates with hyperacetylation. *J Biol Chem* **280**, 38814-38822. (https://doi.org/10.1074/jbc.M505563200)

Towbin BD, Gonzales-Sandoval A, Gasser SM (2013) Mechanisms of heterochromatin subnuclear localization. *Trends Biochem Sci* **38**, 356-363. (https://doi.org10.1016/j.tibs.2013.04.004)

Towbin BD, Meister P, Gasser SM (2009) The nuclear envelope – a scaffold for silencing? *Curr Op Genet Dev* **19**, 180-186. (https://doi.org/10.1016/j.gde.2009.01.006)

Vidal BC, Schlüter G, Moore GW (1973) Cell nucleus pattern recognition: influence of staining. *Acta Cytol* **17**, 510-521.

#1
#2

Wigglesworth VB (1984) *Insect Physiology*, 8th ed.; Chapman and Hall; London.

Wu R, Terry AV, Singh PB, Gilbert DM (2005) Differential subnuclear localization and replication timing of histone H3 lysine 9 methylation states. *Mol Biol Cell* **16**, 2872-2881. (https://doi.org/10.1091/mbc.e04-11-0997)

Zalenskaya IA, Zalensky AO (2004) Non-random positioning of chromosomes in human sperm nuclei. *Chromosome Res* **12**, 163-173. (https://doi.org/10.1023/B:CHRO.0000013166.04629.97)

Competing interests: The authors declare no competing interests.

Legends for figures

Fig. 1. Tri-dimensional model of a structure similar to a Malpighian tubule nucleus of *T. infestans*, as a reference to represent the proximal (p) and distal (d) distances in the X, Y and Z coordinates between a chromocenter body (white c) and the nuclear periphery. The whole nucleus schematic structure (a) and the optical section plans (b, c) are shown.

Fig. 2. Fluorescent Feulgen-stained nuclei of *T. infestans* 5th instar nymphs. The images show part of the galleries that were obtained for single- (a) and multichromocentered (b) nuclei using confocal microscopy. The arrows indicate the chromocenter(s).

Fig. 3. Comparison of the distances in the X, Y and Z axes between the chromocenters and the nuclear periphery in Feulgen-stained cell nuclei of Malpighian tubules of *T. infestans*. Nuclear diameters (axes) were also compared. Vertical lines on the bars indicate the mean standard deviations; horizontal lines in the bars indicate the median values. * and ●, differences significant at $P_{0.05}$ between compared groups. Statistical comparisons are listed in Supplementary Tables 1 and 2. M, multichromocentered nuclei; S, single-chromocentered nuclei.

Fig. 4. FISH with 18S rDNA probe signals (green color) in 5th instar nymphs of *T. infestans*. These signals are especially intense on the surface of the chromocenters.

Video 1. A 3-D view from a fluorescent Feulgen-stained single-chromocentered nucleus of a 5th instar nymph.

Videos 2 and 3. 3-D views from FISH-treated nuclei of *T. infestans* reveal the spatial distribution of the 18S rDNA sites especially with respect to the chromocenters (green color). The preparations were counterstained with DAPI (blue color).

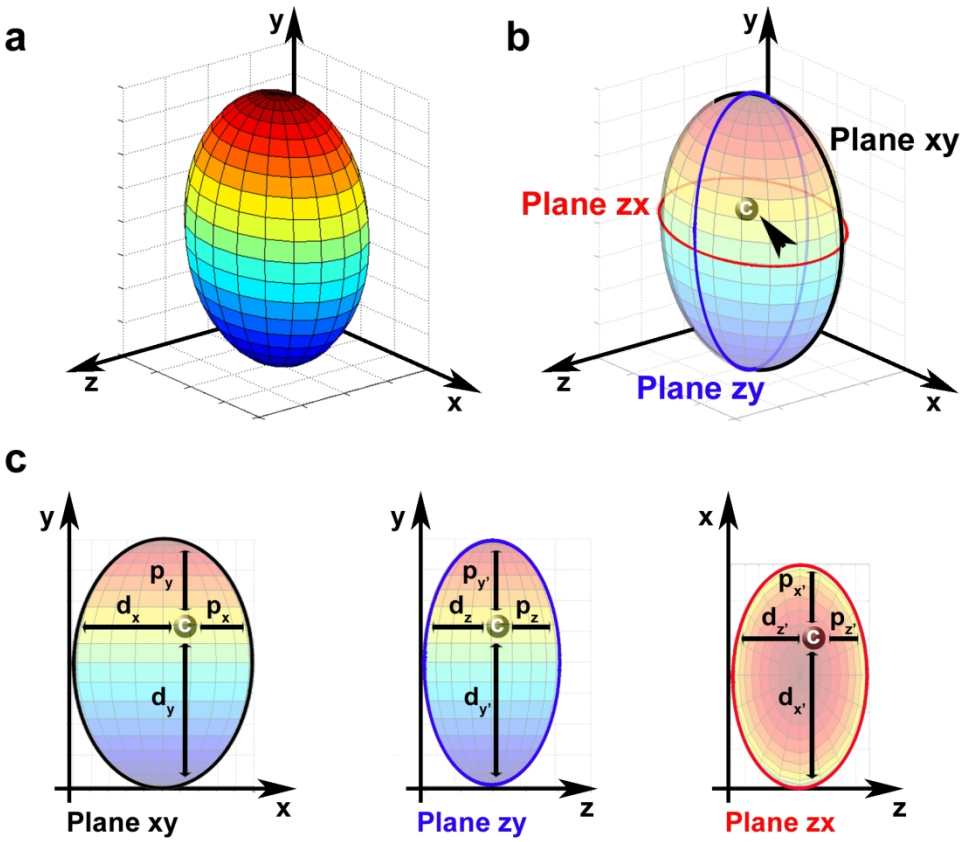

Figure 1

Fig. 1. A tri-dimensional model of a structure similar to a Malpighian tubule nucleus of T. infestans, as a reference to represent the proximal (p) and distal (d) distances in the X, Y and Z coordinates between a chromocenter body (white c) and the nuclear periphery. The whole nucleus schematic structure (a) and the optical section plans (b,c) are shown.

152x146mm (300 x 300 DPI)

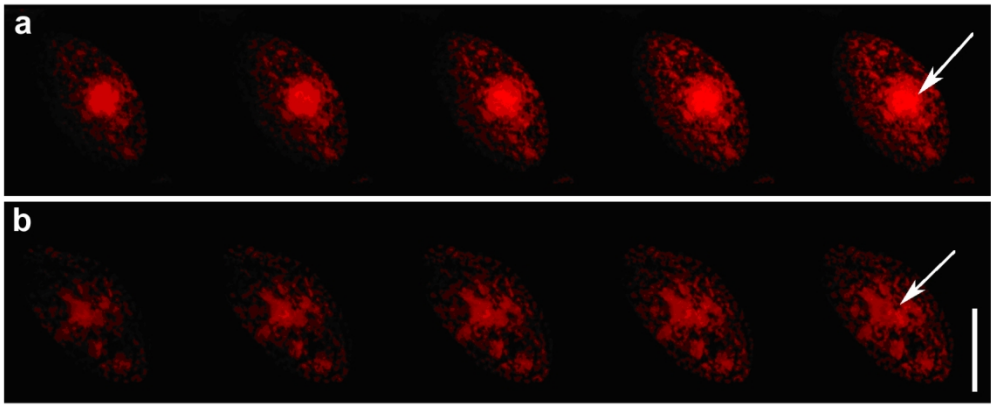

Figure 2

Fig. 2. Fluorescent Feulgen-stained nuclei of T. infestans 5th instar nymphs. The images show part of the galleries that were obtained for single- (a) and multi-chromocentered (b) nuclei using confocal microscopy. The arrows indicate the chromocenter(s).

150x69mm (300 x 300 DPI)

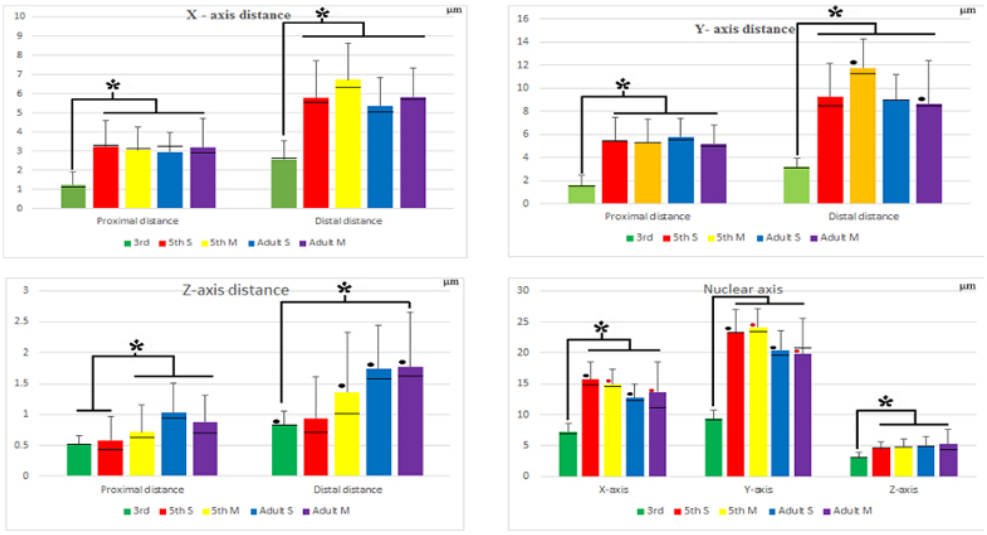

Figure 3

Fig. 3. Comparison of the distances in the X, Y and Z axes between the chromocenters and the nuclear periphery in Feulgen-stained cell nuclei of Malpighian tubules of T. infestans. Nuclear diameters (axes) were also compared. Vertical lines on the bars indicate the mean standard deviations; horizontal lines in the bars indicate the median values. * and •, differences significant at P 0.05 between compared groups. Statistical comparisons are listed in Supplementary Tables 1 and 2. M, multi-chromocentered nuclei; S, single-chromocentered nuclei.

280x164mm (72 x 72 DPI)

Table 1. Proximal and distal distances between the chromocenters and the nuclear periphery in Malpighian tubule cells of *T. infestans*.

Distances (µm)	Axes	3rd instar nymphs Single-chromocentered nuclei (n = 26)			5th instar nymphs Single-chromocentered nuclei (n = 48)			5th instar nymphs Multi-chromocentered nuclei (n = 21)			Adults Single-chromocentered nuclei (n = 19)			Adults Multi-chromocentered nuclei (n = 11)		
		X	SD	CV (%)	X	SD	CV (%)	X	SD	(CV %)	X	SD	(CV %)	X	SD	(CV %)
Proximal	X	1.26	0.70	52.57	3.25	1.32	40.59	3.07	1.17	38.23	2.96	1.00	33.26	3.19	1.51	47.50
	Y	1.62	0.73	44.83	5.41	2.07	38.28	5.30	2.00	37.94	5.79	1.64	28.31	5.15	1.66	32.12
	Z	0.52	0.13	25.65	0.58	0.38	65.90	0.71	0.44	61.40	1.03	0.50	46.88	0.88	0.42	47.60
Distal	X	2.58	0.99	38.44	5.80	1.92	33.14	6.72	1.92	28.68	5.38	1.46	27.19	5.84	1.50	25.52
	Y	3.20	0.90	27.57	9.26	2.90	31.26	11.77	2.50	21.29	9.05	2.14	23.70	8.68	3.73	43.00
	Z	0.83	0.22	26.87	0.93	0.66	71.56	1.31	0.96	70.94	1.75	0.70	40.07	1.76	0.90	50.59
Nuclear diameter	X	7.22	1.35	18.62	15.68	2.86	18.23	14.93	2.40	16.10	12.72	2.21	17.37	13.69	4.80	34.86
	Y	9.37	1.32	14.06	23.27	3.80	16.34	24.16	3.04	12.60	20.47	3.18	15.53	19.84	5.67	28.60
	Z	3.12	0.78	24.90	4.53	1.08	23.85	4.80	1.26	26.70	5.06	1.45	28.72	5.26	2.33	44.43

CV, coefficient of variability; SD, standard deviation; X, arithmetic means

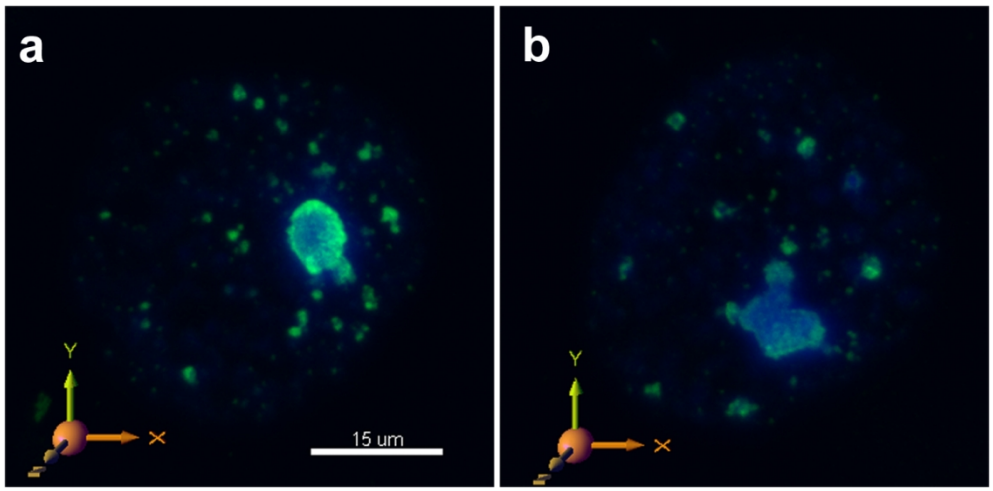

Figure 4

Fig. 4. FISH with 18S rDNA probe signals (green color) in 5th instar nymphs of T. infestans. These signals are especially intense in the surface of the chromocenters.

131x73mm (300 x 300 DPI)

Supplementary Information

Spatial distribution of heterochromatin bodies in the nuclei of *Triatoma infestans* (Klug)

Carlos Henrique L. Imperador[1], Vanessa B. Bardella[2], Eli Heber M. dos Anjos[1], Vera L.C.C. Rodrigues[3], Diogo C. Cabral-de-Mello[2] and Maria Luiza S. Mello[1]

[1] Department of Structural and Functional Biology, Institute of Biology, University of Campinas (Unicamp), Rua Monteiro Lobato 255, 13083-862 Campinas, SP, Brazil; karlosimpe@gmail.com (C.H.L.I.); mlsmello@unicamp.br (M.L.S.M.); eliheber@unicamp.br (E.H.M.A.);

[2] Department of Biology, Institute of Biosciences, State University of São Paulo (Unesp), Avenida 24-A, 1515, 13506-900 Rio Claro, SP, Brazil; vbbardella@gmail.com (V.B.B.); mellodc@rc.unesp.br (D.C.C.M.);

[3] Superintendence for Control of Endemic Diseases (SUCEN), Rua Afonso Pessini, 86, 13845-206 Mogi-Guaçu, SP, Brazil; veracorrea@dglnet.com.br (V.L.C.C.R.)

Author for correspondence: Maria Luiza S. Mello, E-mail: mlsmello@unicamp.br

Table S1. Proximal and distal distances between the chromocenter (s) and the nuclear periphery in Feulgen-stained cell nuclei of Malpighian tubules of *T. infestans* compared in the X-, Y- and Z- optical axes.

Developmental stage	Nuclear phenotype	Parameters	Axis comparison	Test	P	Decision
Nymphal 3rd instar	SC	Proximal distance	X x Y x Z	KW	0.0000	SS
			X x Y	MW	0.0590	NS
			X x Z	MW	0.0000	SS
			Y x Z	MW	0.0000	SS
		Distal distance	X x Y x Z	KW	0.0000	SS
			X x Y	MW	0.0270	S
			X x Z	MW	0.0000	SS
			Y x Z	MW	0.0000	SS
		Nucleus axis	X x Y x Z	KW	0.0000	SS
			X x Y	MW	0.0000	SS
			X x Z	MW	0.0000	SS
			Y x Z	MW	0.0000	SS
Nymphal 5th instar	SC	Proximal distance	X x Y x Z	KW	0.0000	SS
			X x Y	MW	0.0000	SS
			X x Z	MW	0.0000	SS
			Y x Z	MW	0.0000	SS
		Distal distance	X x Y x Z	KW	0.0000	SS
			X x Y	MW	0.0000	SS
			X x Z	MW	0.0000	SS
			Y x Z	MW	0.0000	SS
		Nucleus axis	X x Y x Z	KW	0.0000	SS
			X x Y	MW	0.0000	SS
			X x Z	MW	0.0000	SS
			Y x Z	MW	0.0000	SS
	MC	Proximal distance	X x Y x Z	KW	0.0000	SS
			X x Y	MW	0.0020	SS
			X x Z	MW	0.0000	SS
			Y x Z	MW	0.0000	SS
		Distal distance	X x Y x Z	KW	0.0000	SS
			X x Y	MW	0.0000	SS
			X x Z	MW	0.0000	SS
			Y x Z	MW	0.0000	SS
		Nucleus axis	X x Y x Z	KW	0.0000	SS
			X x Y	MW	0.0000	SS
			X x Z	MW	0.0000	SS
			Y x Z	MW	0.0000	SS

Adult	SC	Proximal distance	X x Y x Z	KW	0.0000	SS
			X x Y	MW	0.0000	SS
			X x Z	MW	0.0000	SS
			Y x Z	MW	0.0000	SS
		Distal distance	X x Y x Z	KW	0.0000	SS
			X x Y	MW	0.0000	SS
			X x Z	MW	0.0000	SS
			Y x Z	MW	0.0000	SS
		Nucleus axis	X x Y x Z	KW	0.0000	SS
			X x Y	MW	0.0000	SS
			X x Z	MW	0.0000	SS
			Y x Z	MW	0.0000	SS
	MC	Proximal distance	X x Y x Z	KW	0.0000	SS
			X x Y	MW	0.0000	SS
			X x Z	MW	0.0000	SS
			Y x Z	MW	0.0000	SS
		Distal distance	X x Y x Z	KW	0.0000	SS
			X x Y	MW	0.0200	S
			X x Z	MW	0.0000	SS
			Y x Z	MW	0.0000	SS
		Nucleus axis	X x Y x Z	KW	0.0000	SS
			X x Y	MW	0.0010	SS
			X x Z	MW	0.0000	SS
			Y x Z	MW	0.0000	SS

KS, Kruskal-Wallis; MC, multi-chromocentered nuclei; MW, Mann-Whitney; NS, non-significant; SC, single-chromocentered nuclei; S, significant; SS, highly significant.

Table S2. Proximal and distal distances between the chromocenter (s) and the nuclear periphery in the X, Y, and Z optical axes in Feulgen-stained cell nuclei of Malpighian tubules of *T. infestans* compared between developmental stages.

Parameters	Developmental stage comparison	Nuclear phenotype	Test	P	Decision
X-axis proximal distance	3rd x 5th instar nymphs x adults	SC	KW	0.0000	SS
	3rd x 5th instar nymphs	SC	MW	0.0000	SS
	3rd instar nymphs x adults	SC	MW	0.0000	SS
	5th instar nymphs x adults	SC	MW	0.6165	NS
		MC	MW	0.9698	NS
X-axis distal distance	3rd x 5th instar nymphs x adults	SC	KS	0.0000	SS
	3rd x 5th instar nymphs	SC	MW	0.0000	SS
	3rd instar nymphs x adults	SC	MW	0.0000	SS
	5th instar nymphs x adults	SC	MW	0.4867	NS
		MC	MW	0.1904	NS
Y-axis proximal distance	3rd x 5th instar nymphs x adults	SC	KW	0.0000	SS
	3rd x 5th instar nymphs	SC	MW	0.0000	SS
	3rd instar nymphs x adults	SC	MW	0.0000	SS
	5th instar nymphs x adults	SC	MW	0.4911	NS
		MC	MW	0.9368	NS
Y-axis distal distance	3rd x 5th instar nymphs x adults	SC	KW	0.0000	SS
	3rd x 5th instar nymphs	SC	MW	0.0000	SS
	3rd instar nymphs x adults	SC	MW	0.0000	SS
	5th instar nymphs x adults	SC	MW	0.9169	NS
		MC	MW	0.0155	S
Z-axis proximal distance	3rd x 5th instar nymphs x adults	SC	KW	0.0000	SS

	3rd x 5th instar nymphs	SC	MW	0.5572	NS
	3rd instar nymphs x adults	SC	MW	0.0000	SS
	5th instar nymphs x adults	SC	MW	0.0002	SS
		MC	MW	0.0131	S
Z-axis distal distance	3rd x 5th instar nymphs x adults	SC	KW	0.0000	SS
	3rd x 5th instar nymphs	SC	MW	0.4395	NS
	3rd instar nymphs x adults	SC	MW	0.0000	SS
	5th instar nymphs x adults	SC	MW	0.0001	SS
		MC	MW	0.1532	SS
Nucleus X-axis	3rd x 5th instar nymphs X adults	SC	KW	0.0000	SS
	3rd x 5th instar nymphs	SC	MW	0.0000	SS
	3rd instar nymphs x adults	SC	MW	0.0000	SS
	5th instar nymphs x adults	SC	MW	0.0001	SS
		MC	MW	0.1218	NS
Nucleus Y-axis	3rd x 5th instar nymphs x adults	SC	KW	0.0000	SS
	3rd x 5th instar nymphs	SC	MW	0.0000	SS
	3rd instar nymphs x adults	SC	MW	0.0000	SS
	5th instar nymphs x adults	SC	MW	0.0063	SS
		MC	MW	0.0391	S
Nucleus Z-axis	3rd x 5th instar nymphs x adults	SC	KW	0.0000	SS
	3rd x 5th instar nymphs	SC	MW	0.0000	SS
	3rd instar nymphs x adults	SC	MW	0.0000	SS
	5th instar nymphs x adults	SC	MW	0.3622	NS
		MC	MW	0.9368	NS

KS, Kruskal-Wallis; MC, multi-chromocentered nuclei; MW, Mann-Whitney; NS, non-significant; SC, single-chromocentered nuclei; S, significant; SS, highly significant.

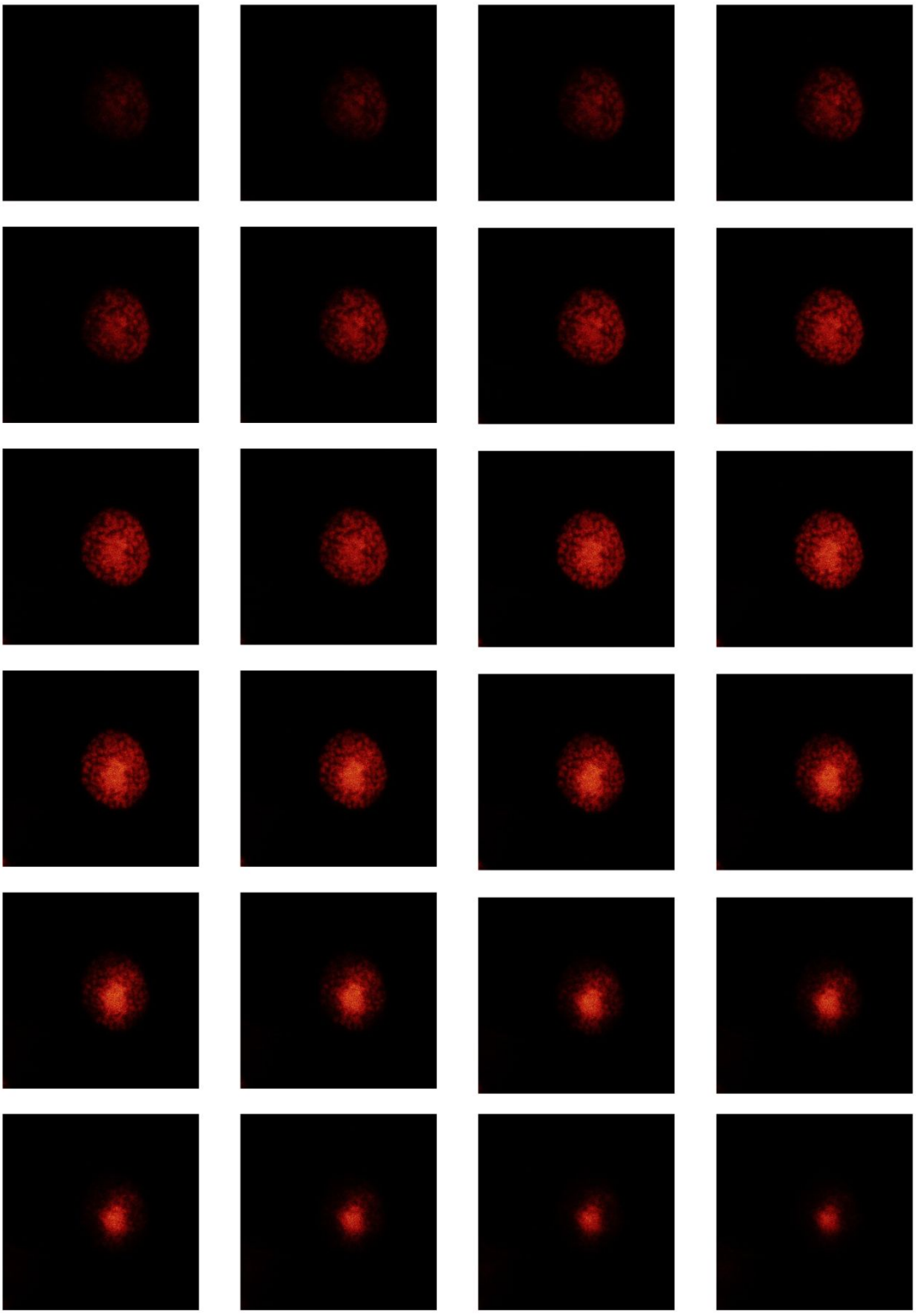

Fig. S1. Example of a gallery composed of confocal microscopy optical sections of a Feulgen-stained Malpighian tubule cell nucleus from a single-chromocentered 3rd instar nymph of *T. infestans*.

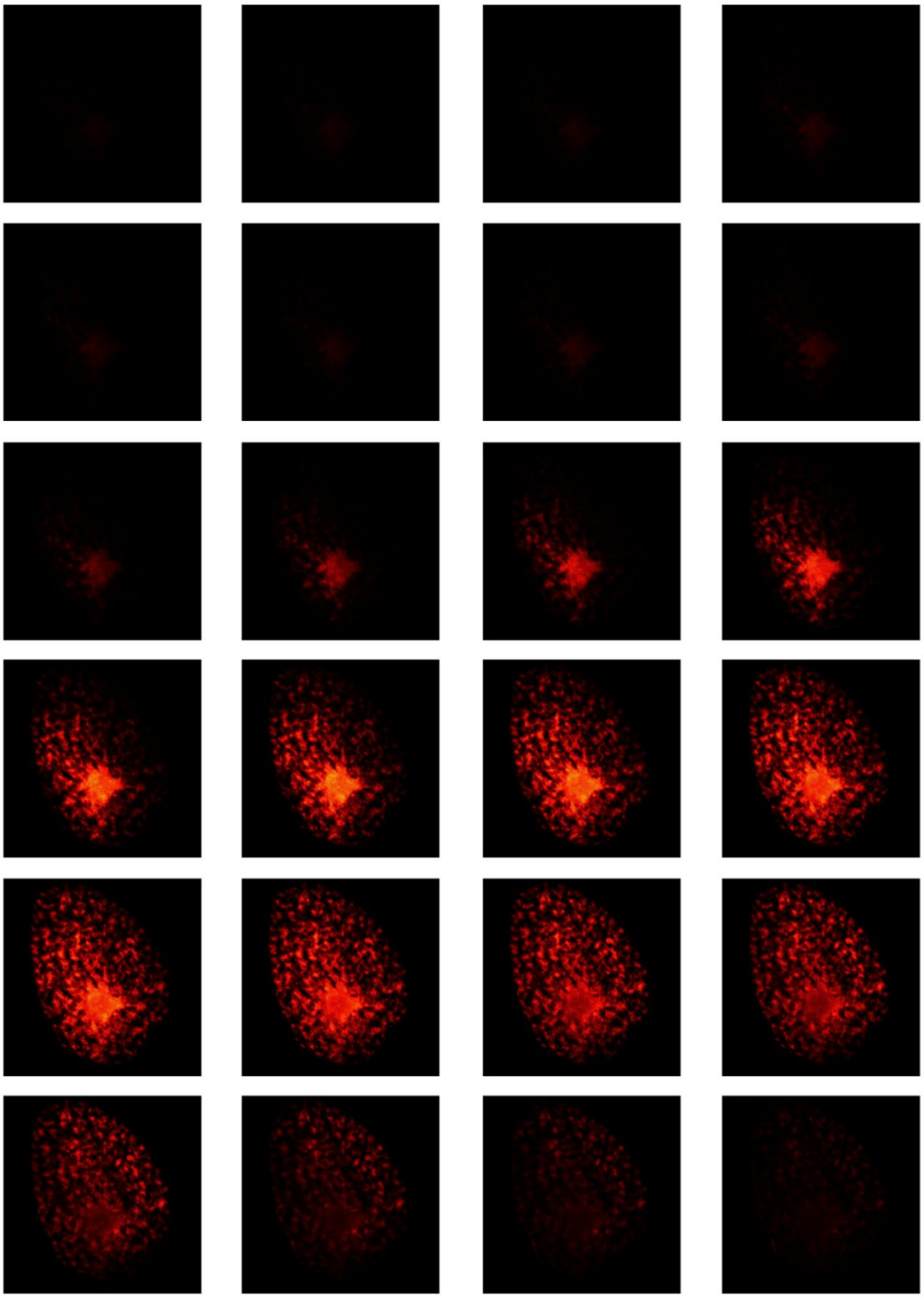

Fig. S2. Example of a gallery composed of confocal microscopy optical sections of a Feulgen-stained Malpighian tubule single-chromocentered cell nucleus from a 5th instar nymph of *T. infestans*.

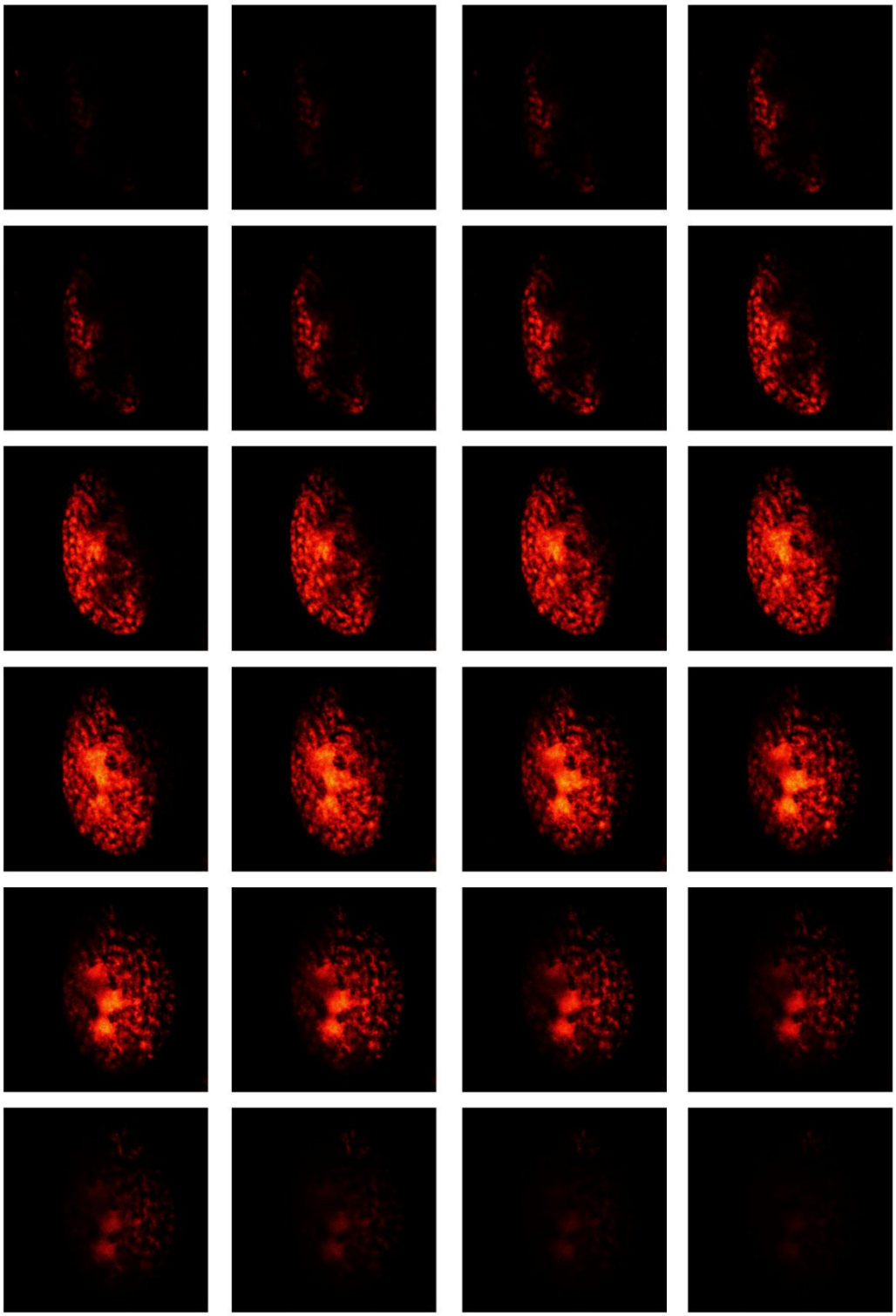

Fig. S3. Example of a gallery composed of confocal microscopy optical sections of a Feulgen-stained Malpighian tubule multi-chromocentered cell nucleus from a 5th instar nymph of *T. infestans*.

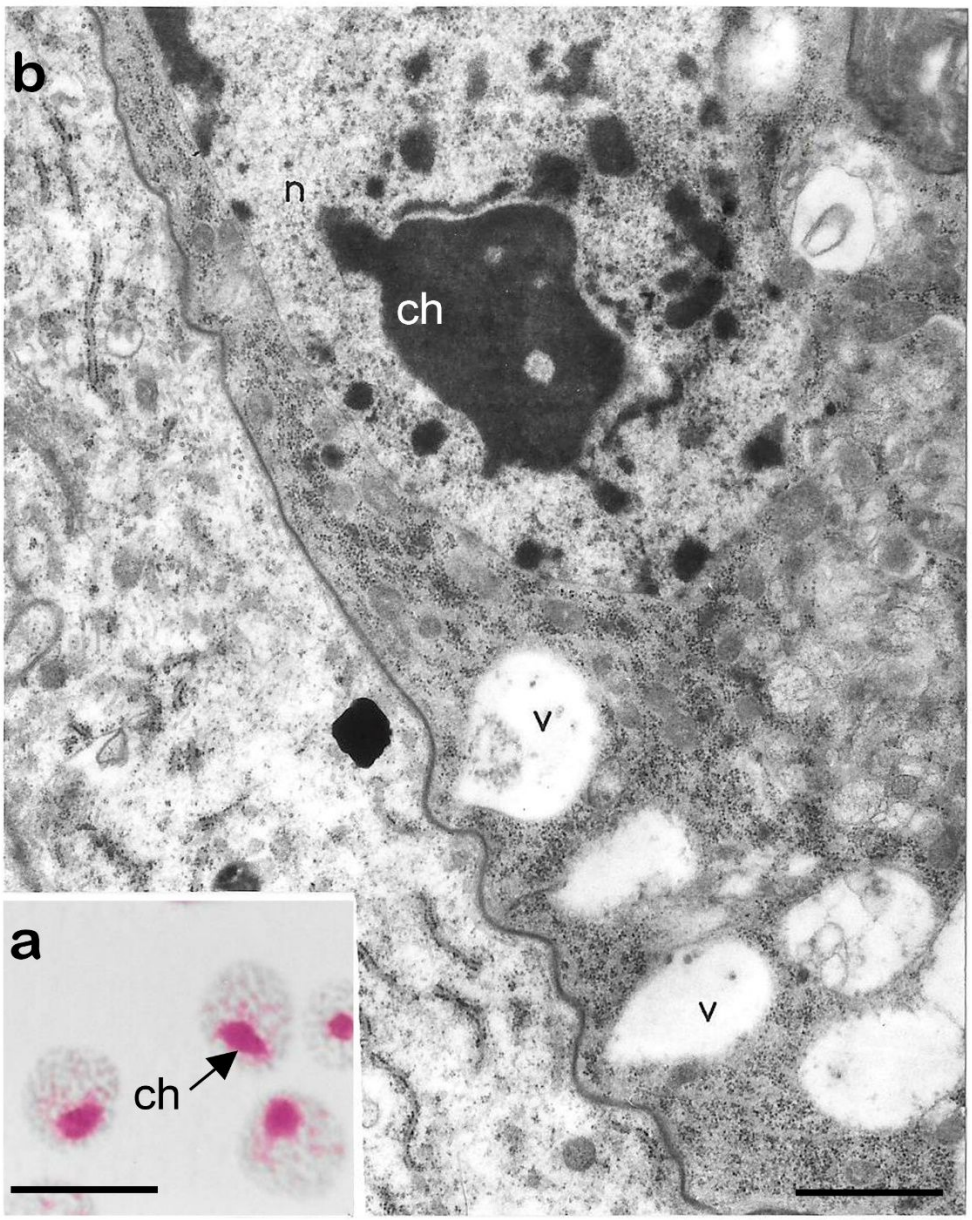

Fig. S4. Proximity of the chromocenter to the nuclear periphery in cells of *T. infestans*. a. A Feulgen-stained nucleus. b. Ultrastructural image of Malpighian tubule cells fixed in phosphate buffered 3% glutaraldehyde at pH 7.2 for 3 h, postfixed in phosphate buffered 1% osmium tetroxide for one hour, embedded in Epon 812, and stained with uranyl acetate and lead citrate. Observation made with a Zeiss EM 9 electron microscope. (Mello MLS, Dolder H). ch, chromocenter; n, nucleus; v, cytoplasmic vesicle. Bars equal to 20 µm (a) and 1 µm (b).

#1
#2